Planar bootstrap without the dual-tree approximation

Louis A. P. Balázs*
Fermi National Accelerator Laboratory,† Batavia, Illinois 60510
and Physics Department, Purdue University, West Lafayette, Indiana 47907
(Received 24 January 1977)

We consider a dual multiperipheral model at and near $t = 0$, and argue that the usual imposition of a Regge-cluster finite-energy sum rule is probably redundant. Instead we require that the $\pi\pi$ amplitude satisfy the Adler PCAC (partial conservation of axial-vector current) condition and crossing near $s = t = 0$. We then set up a specific Padé approximation to the multiperipheral model. This becomes exact for a factorizable model, but takes into account transverse-momentum effects and explicitly incorporates the deferred thresholds arising from the production of clusters. We do not make the dual-tree approximation for our Reggeon couplings, which we represent instead by a more general exponential form. If we then assume a linear Reggeon trajectory $\alpha(t)$, self-consistency gives an intercept $\alpha(0) = 0.49$ and a triple-Regge coupling which is in reasonable agreement with experiment. There are no arbitrary parameters in our model.

I. INTRODUCTION

The first step in any strong-interaction dual-unitarization program, such as the Veneziano $1/N$ expansion,[1,2] is the "planar bootstrap."[3] This is a self-consistent calculation of exchange-degenerate Reggeon poles based on planar unitarity, and is unaffected by Regge-cut corrections, fixed poles, diffraction, and absorption.[4] One then adds in corrections (cylinder, torus, etc.) which bring in a Pomeron and its interaction with the Reggeon and with itself.[2,5]

Planar bootstrap calculations are generally carried out within a cluster multiperipheral-model framework. In addition, we normally have the following:

(i) Rather simple kinematics is usually assumed. This does not take into account threshold and transverse-momentum effects which are known to be important in certain problems.[6,7]

(ii) Clusters are related to Regge exchange using either explicit finite-energy sum rules[8] or local duality.[2] We shall argue that such a procedure may sometimes be redundant.

(iii) Unless the planar bootstrap is used merely to fix certain parameters for cylinder and torus calculations, the dual-tree approximation generally has to be made for Regge couplings.[3,9] It would be desirable to do a calculation in which as many coupling properties as possible are determined by the bootstrap itself.

In the present paper we set up a model in which the above three difficulties do not arise. In previous planar bootstrap calculations crossing was only applied in a very limited way. In the present calculation we shall apply it directly in the neighborhood of $s = t = 0$. At the same time we require that the $\pi\pi$ amplitude satisfy the Adler PCAC (partial conservation of axial-vector current) condition. If we then assume a linear Reggeon trajectory and a general exponential form for our Regge couplings we find that we can calculate all the parameters of our model.

In Sec. II we review the dual multiperipheral model. In Sec. III we discuss the Adler PCAC condition[10] and crossing near $s = t = 0$. In Sec. IV we discuss a Padé approximation to the multiperipheral model. This involves a box graph, which is evaluated in Sec. V. In Sec. VI we write down our bootstrap results and compare them with the dual-tree approximation. In Sec. VII we include cylinder corrections and calculate the parameters of the Pomeron at intermediate energies. These are then compared with experiment. Finally, in the Appendixes we discuss various multiperipheral models in detail, and, in particular, the conditions under which a Padé approximation may be valid.

II. DUAL MULTIPERIPHERAL MODEL

In the multiperipheral cluster-production model, the absorptive part for a two-body process is given by a sum of ladder graphs (Fig. 1). The vertical lines are narrow-resonance clusters a of mass $\sqrt{s_a}$. It was argued in Ref. 6 that only a single meson cluster, with $s_a \simeq 0.5$ GeV^2 and corresponding to the ρ, ω, ϵ, ... peaks, is expected to be important at the sort of intermediate energies where Reggeons play any important role and where duality considerations are expected to apply. In a dual multiperipheral model the horizontal lines are linear combinations of exchange-degenerate pairs of Regge exchanges α.

(A) At the planar bootstrap level we only have uncrossed (planar) quark-duality diagrams of the type shown in Fig. 2. The exchanges then correspond to Regge propagators

$$R = e^{-i\pi\alpha(t)} s^{\alpha(t)} . \tag{2.1}$$

We will assume that SU(3) is exact so that the ρ-A_2, K^*-K^{**}, ω-f, and ϕ-f' pairs are all degenerate, with a linear trajectory

$$\alpha(t) = \alpha_0 + \alpha' t . \tag{2.2}$$

All possible quark diagrams have equal weight.

If we are interested in generating the Pomeron, we must include in the sum of Fig. 1 crossed (cylinder) loops of the type shown in Fig. 3, in addition to the uncrossed loops of Fig. 2. In the former case we then have a Regge propagator

$$R = 1 s^{\alpha(t)} . \tag{2.3}$$

(B) In order to obtain an additional constraint on the couplings, the assumption is usually made that the clusters are dual in a finite-energy sum-rule sense to Regge behavior. (See Fig. 4, where the external lines would be either Reggeons or particles.) This kind of constraint on sums of ladder graphs was first used a number of years ago within a pion-exchange model[8] and has recently been applied extensively in the dual multiperipheral apprach,[3,4] often in the extreme local-duality limit.[2] If Γ_a represents the coupling of the cluster a to the external lines of Fig. 4, we have a relation of the form

$$\Gamma_a = F_a g_1 g_2 , \tag{2.4}$$

where F_a is a purely kinematic factor. We shall argue in Appendix A that F_a has approximate factorization properties. This in turn means that Γ_a likewise factorizes.

Explicit expressions for F_a can be obtained from finite-energy sum rules (FESR's). However, there are two difficulties which then arise.

(i) An explicit FESR involves a separation point between low and high energies which is only known approximately.

(ii) Since Fig. 1 itself has the correct analyticity properties and gives Regge behavior for high s, our multiperipheral model already relates the cluster of Fig. 1(a) to Regge behavior. Thus any further application of an explicit FESR to the overall amplitude A of Fig. 1 is redundant and may even lead to difficulties. At best it may be a crude

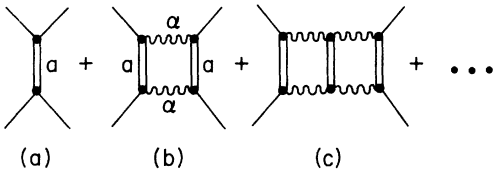

FIG. 1. Absorptive part for a multiperipheral cluster model.

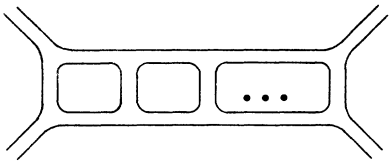

FIG. 2. Uncrossed (planar) quark-duality diagram.

and indirect way of imposing corssing, since crossing-symmetric dual amplitudes are known to satisfy simple FESR's. However, a better procedure would be to avoid an explicit FESR altogether in this case and impose crossing directly instead. This will be discussed in the next section.

III. ADLER ZERO AND CROSSING

Suppose we consider $\pi\pi$ scattering for simplicity, with $m_\pi{}^2 \approx 0$. Adler's self-consistency condition[10] then requires that the amplitude

$$T(s=0, t=0) = 0 . \tag{3.1}$$

Now the planar amplitude satisfies a fixed-t dispersion relation

$$T(s,t) = \frac{1}{\pi} \int_{4m_\pi{}^2}^{\infty} ds' \, \frac{A(\nu', t)}{\nu' - \nu} , \tag{3.2}$$

where $\nu = \frac{1}{2}(s-u) \simeq s + \frac{1}{2}t$ is the usual crossing-symmetric variable used in finite-energy sum rules. If we expand in ν,

$$\pi T(s,t) = \sum_{l=0}^{\infty} \nu^l A_l(t) , \tag{3.4}$$

where

$$A_l(t) = \int_{4m_\pi{}^2}^{\infty} ds' \nu'^{-l-1} A(\nu', t) . \tag{3.4}$$

At $t=0$ this coincides with the usual Mellin transform. We shall see in Sec. IV that it also arises naturally for $t \neq 0$. If we follow Lovelace[11] and apply Eq. (3.1) to Eq. (3.3) we obtain

$$A_0(0) = 0 . \tag{3.5}$$

Further constraints can be obtained by combining Eq. (3.4) with the planar crossing condition

$$T(s,t) = T(t,s) . \tag{3.6}$$

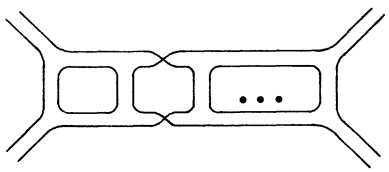

FIG. 3. Nonplanar (cylinder) quark-duality diagram with crossed and uncrossed loops.

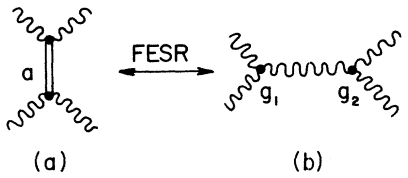

FIG. 4. Average duality relation between cluster (a) and Reggeon (b).

In particular the relation

$$T(0,t)=T(t,0)\,, \tag{3.7}$$

which relates the amplitude along the lines $s=0$ and $t=0$ in Fig. 5, gives the relations

$$A_0'(0)=\tfrac{1}{2}A_1(0),\ldots\,. \tag{3.8}$$

From Fig. 1(a) we have a contribution to the absorptive part

$$W(s,t)=\Gamma(t)\delta(s-s_a)\,. \tag{3.9}$$

Figures 1(b), 1(c),..., on the other hand, give rise to approximate Regge behavior. We can therefore make the usual FESR assumption that

$$A(s,t)\simeq W(s,t),\quad s<N_0 \tag{3.10}$$

$$\simeq b(t)\nu^{\alpha(t)},\quad s>N_0 \tag{3.11}$$

where N_0 is midway between s_a and the next cluster above it. If we take both of these to lie on the trajectory (2.2) we then have

$$N_0\alpha'=1.5-\alpha_0\,, \tag{3.12}$$

where

$$\alpha'=(1-\alpha_0)/s_a\,. \tag{3.13}$$

If we now insert Eqs. (3.10) and (3.11) into Eq. (3.2) and impose the conditions (3.1) and (3.7) we obtain

$$\Gamma(t)=F(t)b(t)\,, \tag{3.14}$$

where, for small t,

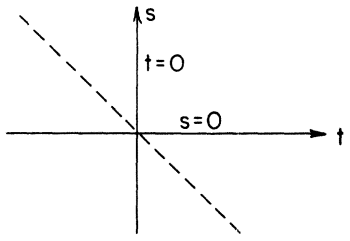

FIG. 5. Mandelstam diagram illustrating planar $s-t$ crossing.

$$F(t)=N_0{}^{\alpha_0}\frac{s_a}{\alpha_0}\left\{1+\alpha' t\left[\ln N_0+\frac{\alpha_0}{2\alpha' N_0}+\frac{1}{\alpha' s_a}-\frac{1}{\alpha_0}-\frac{\alpha_0}{2}\frac{(\alpha' N_0)^{-1}}{\alpha_0-1}\right]+\cdots\right\}. \tag{3.15}$$

We will use this constraint instead of Eq. (2.4) in what follows.

IV. PADÉ APPROXIMATION

Let us consider the usual Froissart-Gribov projection of Eq. (3.2)

$$T_l(t)=\frac{1}{2\pi q_t{}^2}\int_{4m_\pi{}^2}^{\infty}ds'A(s',t)Q_l\left(1+\frac{s'}{2q_t{}^2}\right), \tag{4.1}$$

where $q_t{}^2=\frac{1}{4}t-m_\pi{}^2$ and A is normalized so that

$$A(s,0)=\lambda^{1/2}(s,m_\pi{}^2,m_\pi{}^2)\sigma_{\rm tot}(s)\,, \tag{4.2}$$

with $\lambda(x,y,z)=x^2+y^2+z^2-2(xy+yz+zx)$. For small t, we can make the asymptotic approximation

$$Q_l(z)=B(l+1,\tfrac{1}{2})(2z)^{-l-1}\,, \tag{4.3}$$

where B is the usual Euler beta function. A combination which is free of kinematic singularities in t is then

$$2\pi B^{-1}(l+1,\tfrac{1}{2})q_t{}^{-2l}T_l(t)\simeq A_l(t)\,, \tag{4.4}$$

where $A_l(t)$ is defined as in Eq. (3.4). If we apply this projection to Eq. (3.9), for example, we obtain

$$W_l(t)=\Gamma(t)(s_a+\tfrac{1}{2}t)^{-l-1}\,. \tag{4.5}$$

If the sum of Fig. 1 is treated as an expansion

$$A_l(t)=W_l(t)+B_l(t)+\cdots\,, \tag{4.6}$$

the [1,1] Padé approximant has the form[9,12]

$$[1,1]=W_l(t)/D_l(t)\,, \tag{4.7}$$

where

$$D_l(t)=1-B_l(t)/W_l(t) \tag{4.8}$$

and B_l is the contribution of Fig. 1(b).

An advantage of the "diagonal" $[N,N]$ Padé approximants is that they satisfy a version of t-channel unitarity in which the particles lying on the exchanged Reggeon trajectories appear in the intermediate state.[13] If we include π exchange along with the Regge exchanges of Fig. 1, these approximants also satisfy elastic t-channel unitarity exactly in the elastic region. Furthermore, in the case of a factorizable multiperipheral model, it is simple to show that the [1,1] approximant is in fact exact.[9]

The practical advantage of using the [1,1] Padé approximant is that we only have to evaluate the first two diagrams of Fig. 1 explicitly. We do

not have to first set up a full-fledged multiperipheral integral equation.

V. BOX GRAPH NEAR THE FORWARD DIRECTION

We will assume that the coupling Γ_a in Fig. 6 factorizes so that we can write

$$\Gamma_a = \gamma^*_{\pi a\alpha}(t'', t)\gamma_{\pi a\alpha}(t', t)\,. \tag{5.1}$$

In the forward direction, Fig. 1(b) then gives

$$B(s,0) = \frac{1}{16\pi s}\int_{t_-}^{t_+} dt'\,|T_R(t',0)|^2\theta(s-4s_a)\,, \tag{5.2}$$

where θ is the usual step function,

$$t_\pm \simeq -\tfrac{1}{4}[s^{1/2} \mp (s-4s_a)^{1/2}]^2 \tag{5.3}$$

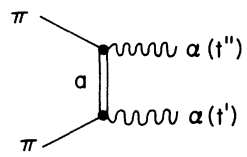

FIG. 6. Coupling of cluster to pions and Reggeons.

in the limit of small $m_\pi{}^2$, and

$$T_R(t',t) = \gamma_{\pi a\alpha}{}^2(t',t)X(t')(\alpha' s)^{\alpha(t')}\,, \tag{5.4}$$

with

$$X(t) = e^{-i\pi\alpha(t)}/\sin\pi\alpha(t)\,. \tag{5.5}$$

Figure 1(b) also gives

$$\left[\frac{\partial B(s,t)}{\partial t}\right]_{t=0} = \frac{1}{16\pi s}\int_{t_-}^{t_+} dt'\left\{\left[\frac{\partial}{\partial t}\,|T_R(t',t)|^2\right]_{t=0} - \frac{(t'-t_+)(t'-t_-)}{s}\left|\frac{\partial T_R(t',0)}{\partial t'}\right|^2\right\}\theta(s-4s_a)\,. \tag{5.6}$$

We will see later how $\gamma_{\pi a\alpha}$ can be related to the $\alpha\alpha\alpha$ triple-Regge coupling. For the present we shall simply parametrize it as

$$|X(t')|^2\gamma_{\pi a\alpha}{}^2(t',t) = G^{1/2}e^{At'}e^{ct/2}\,, \tag{5.7}$$

where G, A, and c will all be determined eventually by our bootstrap conditions. Equations (5.2) and (5.6) can now be evaluated to give

$$B(s,0) = \frac{1}{16\pi s}\,\frac{G}{\tilde{A}}\,(\alpha' s)^{2\alpha_0}E_0 \tag{5.8}$$

and

$$\left[\frac{\partial B(s,t)}{\partial t}\right]_{t=0} = cB(s,0) + \frac{1}{16\pi s}\,G\tilde{J}(\alpha' s)^{2\alpha_0}E_1\,. \tag{5.9}$$

where

$$\tilde{A} = 2[A + \alpha'\ln(\alpha' s)]\,, \tag{5.10}$$

$$J = \tfrac{1}{4} + (\alpha'\pi/\tilde{A})^2\,, \tag{5.11}$$

$$E_0 = 2e^{\tilde{A}t_1}\sinh\tilde{A}t_2\,, \tag{5.12}$$

$$E_1 = 4e^{\tilde{A}t_1}(\tilde{A}t_2\cosh\tilde{A}t_2 - \sinh\tilde{A}t_2)/(\tilde{A}s)\,, \tag{5.13}$$

and

$$t_{1,2} = \tfrac{1}{2}(t_+ \pm t_-)\,. \tag{5.14}$$

To simplify our expressions further we could make the approximations

$$E_0 \simeq (1-4s_a/s)^{1/2}\,, \tag{5.15}$$

$$E_1 \simeq (1-4s_a/s)^{3/2}\,, \tag{5.16}$$

which are exact for large s and have the correct type of threshold behavior as $s \to 4s_a$. They are still rather unwieldy, however, and so we will instead make the cruder approximations

$$E_0 \simeq \theta(s - s_{L0})\,, \tag{5.17}$$

$$E_1 \simeq \theta(s - s_{L1})\,, \tag{5.18}$$

where $s_{L0} = 5.333s_a$ and $s_{L1} = 10.81s_a$ are the values of s where Eqs. (5.15) and (5.16) attain their maximum values. At the same time we will "exponentiate" $\tilde{A}$ and J,

$$\tilde{A} \simeq \tilde{A}_{L0}(s/s_{L0})^{2\alpha'/\tilde{A}_{L0}} \tag{5.19}$$

$$J \simeq J_{L1}(s/s_{L1})^{-H_{L1}}\,, \tag{5.20}$$

so that the value and s derivative is exact at $s = s_{L0}$ and $s = s_{L1}$, respectively. Thus

$$\tilde{A}_{Li} = (\tilde{A})_{s=s_{Li}}\,, \tag{5.21}$$

$$J_{L1} = (J)_{s=s_{L1}}\,, \tag{5.22}$$

and

$$H_{L1} = \frac{4}{\pi}(\alpha'\pi/\tilde{A}_{L1})^3 J_{L1}{}^{-1}\,. \tag{5.23}$$

If we now make the partial-wave projection (3.4), we obtain

$$B_l(0) = \frac{G\alpha'^{2\alpha_0}}{16\pi\tilde{A}_{L0}}\,\frac{s_{L0}{}^{2\alpha_0-1-l}}{l+1-2\alpha_0+2\alpha'/\tilde{A}_{L0}} \tag{5.24}$$

and

$$\left[\frac{\partial}{\partial t}\ln B_l(t)\right]_{t=0} = c + \left(l+1-2\alpha_0+\frac{2\alpha'}{\tilde{A}_{L0}}\right)\left[\tilde{A}_{L0}J_{L1}\,\frac{(s_{L1}/s_{L0})^{2\alpha_0-1-l}}{l+1-2\alpha_0+H_{L1}} - \frac{\tfrac{1}{2}(l+1)s_{L0}{}^{-1}}{l+2-2\alpha_0+2\alpha'/\tilde{A}_{L0}}\right]. \tag{5.25}$$

VI. BOOTSTRAP RESULTS AND COMPARISON WITH THE DUAL TREE

Eq. (4.7) has an output pole at $l=\alpha(t)$ if

$$D_{\alpha(t)}=0\,. \tag{6.1}$$

The corresponding residue is then

$$b(t)=W_{\alpha(t)}(t)[\partial D_l(t)/\partial l]_{l=\alpha(t)}^{-1}\,. \tag{6.2}$$

We will only consider the value and t derivative at $t=0$ and require that this output pole be consistent with the input as given by Eqs. (4.5), (3.14), and (2.2). If $\gamma_{\pi\pi\alpha}{}^2=\alpha'^{-\alpha}b$ we then obtain

$$\alpha_0=0.49,\quad G^{1/2}=34.6\,\gamma_{\pi\pi\alpha}(0),$$
$$A=1.99,\quad c=0.12\,. \tag{6.3}$$

Our value of α_0 is in good agreement with experiment.

There is no direct unambiguous way of comparing G, A, and c with experiment. To relate $\gamma_{\pi a\alpha}$ to the $\alpha\alpha\alpha$ triple-Regge coupling g we will use the usual finite-mass sum rule for the inclusive process $\pi\pi\to\pi X$,

$$\int_0^{\bar N_0{}^2} d\bar M^2\left[\frac{d\sigma}{dt'dM^2}-\left(\frac{d\sigma}{dt'dM^2}\right)_R\right]=0\,, \tag{6.4}$$

with

$$\left(\frac{d\sigma}{dt'dM^2}\right)_R=\frac{1}{16\pi s^2}\,\gamma_{\pi\pi\alpha}{}^2(t')\,|X(t')|^2 g(t',t',0)\times\gamma_{\pi\pi\alpha}(0)(s/\bar M^2)^{2\alpha(t')}(\alpha'\bar M^2)^{\alpha(0)}\,, \tag{6.5}$$

where $\bar N_0{}^2=N_0{}^2-m_\pi{}^2-t'$, $\bar M^2=\bar M^2-m_\pi{}^2-t'$, and M is the missing mass (see Fig. 7). We will assume that the low-M^2 region is dominated by the production of the cluster a so that in the narrow-resonance approximation

$$\frac{d\sigma}{dt'dM^2}=\left(\frac{d\sigma}{dt'}\right)_a\delta(M^2-s_a)\,, \tag{6.6}$$

where $(d\sigma/dt')_a$ is the usual differential cross section for $\pi\pi\to\pi a$, which is given by

$$\left(\frac{d\sigma}{dt'}\right)_a=\frac{1}{16\pi s^2}\,\gamma_{\pi\pi a}{}^2(t')\,|X(t')|^2\times\gamma_{\pi a\alpha}{}^2(t')(\alpha' s)^{2\alpha(t')}\,. \tag{6.7}$$

From Eqs. (6.4)–(6.7) we obtain

$$g(t',t',0)=\alpha'\,\frac{\gamma_{\pi a\alpha}{}^2(t')}{\gamma_{\pi\pi a}(0)}\,\frac{\alpha(0)+1-2\alpha(t')}{(\bar N_0{}^2\alpha')^{\alpha(0)+1-2\alpha(t')}}\,. \tag{6.8}$$

This quantity is still difficult to compare with experiment. If we relate it to the *fff* coupling g_c normalized as in Ref. 2 we obtain $g_c\approx 11$ at $t'=0$. This should be compared with the "experimental" estimate $g_c\approx 6.3$ obtained in Ref. 2. However, our calculated value will be lower if we include pion exchange as in Ref. 9. Moreover, the estimate of Ref. 2 relies heavily on a version of two-component duality which may not be valid. In the next section we will consider a less ambiguous confrontation with experiment.

We can also compare our results with the dual-tree approximation, which gives

$$|X(t')|^2 g(t',t',t)=N\bar g^2\,\frac{\Gamma(\alpha(t))\Gamma^2(1-\alpha(t'))}{\Gamma^2(1+\alpha(t)-2\alpha(t'))}\,, \tag{6.9}$$

where $N=3$ if we assume that SU(3) is the underlying group. We then obtain $N\bar g^2/16\pi=3.53$, which is again somewhat larger than the usual value. If we use the dual tree to calculate A and c by expanding Eqs. (6.9), (6.8), and (5.7) in t' and t around $t'=0$ and $t=0$, we obtain $A=1.51$ and $c=-1.61$. This should be compared with the bootstrap values obtained in Eq. (6.3). We see that the value of A is relatively close but that c is quite different.

VII. POMERON PARAMETERS AND COMPARISON WITH EXPERIMENT

As discussed in Sec. II, the Pomeron can be calculated by adding in the cylinder loops of Fig. 3. Thus, we must make the replacement

$$B_l(t)\to\hat B_l(t)=B_l(t)+B_l^x(t)\,, \tag{7.1}$$

in Eq. (4.8), where B_l^x has the same form as B_l except that we must make the replacement

$$X(t)\to X^x(t)=1/\sin\pi\alpha(t) \tag{7.2}$$

in Eq. (5.5). This leads to

$$B_l^x(0)=B_l(0)\,. \tag{7.3}$$

On the other hand, Eq. (5.9) must be replaced by

$$\left[\frac{\partial B^x(s,t)}{\partial t}\right]_{t=0}=cB^x(s,0)+\frac{1}{64\pi s}\,G(\alpha' s)^{2\alpha_0}E_1\,. \tag{7.4}$$

If we use the approximations of Sec. V we then obtain

$$\left[\frac{\partial}{\partial t}\ln B_l^x(t)\right]_{t=0}=c+\left(l+1-2\alpha_0+\frac{2\alpha'}{\tilde A_{L0}}\right)\left[\frac{\tilde A_{L0}}{4}\,\frac{(s_{L1}/s_{L0})^{2\alpha_0-1-l}}{l+1-2\alpha_0}-\frac{\frac{1}{2}(l+1)s_{L0}{}^{-1}}{l+2-2\alpha_0+2\alpha'/\tilde A_{L0}}\right]\,. \tag{7.5}$$

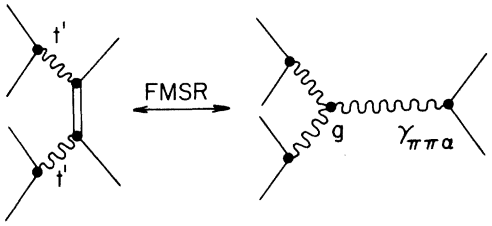

FIG. 7. Finite-mass sum rule for $\pi\pi \to \pi X$ relating the cluster-production and triple-Regge regions.

(A) From Eqs. (6.1) and (6.2) we now obtain, for small t,

$$\alpha_{\hat{P}} = 0.75 + 0.97t, \tag{7.6}$$

$$b_{\hat{P}}/b_f = 1.31(1 - 0.34t). \tag{7.7}$$

The f itself becomes extinct in this calculation. Our "Pomeron" $\hat{P}$, of course, is only an effective pole which describes the cross section for $s \lesssim 50$. To obtain the correct (bare) Pomeron which describes scattering at higher energies, we would have to include higher-mass clusters.[6,14] Our intercept is somewhat lower[15,5,9] and our trajectory slope is larger[2,6] than in other calculations, but should not be inconsistent with the data for $s \lesssim 50$ GeV^2. (See Fig. 4 of Ref. 16.)

The ratio of Eq. (7.7) is the one for $\pi\pi$ scattering. For pp scattering we must make a correction to take into account the fact that the mass of the end cluster $m_N \neq \sqrt{s_a}$. From Ref. 6 or Appendix C we have

$$(b_{\hat{P}}/b_f)_{pp} = (m_N^2/s_a)^{2(\alpha - \alpha_{\hat{P}})} (b_{\hat{P}}/b_f)_{\pi\pi}. \tag{7.8}$$

If we assume that the end cluster is the nucleon, we have $m_N \simeq 1$ GeV. The resulting $b_{\hat{P}}$ is similar to the one obtained in Refs. 6 and 9 and is consistent with the data within the usual large diffractive-correction uncertainties. If we assume $\hat{P}$ and ω exchange, with ω exchange-degenerate with the f, Eqs. (7.6), (7.7), and (7.8) give an essentially constant total pp cross section in the range $10 \lesssim s \lesssim 50$ GeV^2.

(B) We can calculate the average cluster multiplicity from the general formula

$$\langle n \rangle_{\text{cluster}} = \phi\left(\frac{1}{b_{\hat{P}}}\frac{\partial b_{\hat{P}}}{\partial \phi} + \frac{\partial \alpha_{\hat{P}}}{\partial \phi} \ln s\right), \tag{7.9}$$

where ϕ is the same parameter as in Sec. IV (see Appendix C). If we use Eqs. (6.1), (6.2), and (7.8), we obtain

$$\langle n \rangle_{\text{cluster}} = 0.85 + 0.39 \ln s \tag{7.10}$$

for pp scattering. The coefficient of $\ln s$ is much smaller than the usual experimental value. On the other hand, it must be remembered that our result is valid only for $s \lesssim 50$ GeV^2. For higher s additional clusters are produced and we may have a more rapid overall energy dependence. At $s = 20$ GeV^2, Eq. (7.10) gives $\langle n \rangle_{\text{cluster}} \simeq 2$. If we assume 2–3 particles/cluster, i.e., 1.3–2 charged particles/cluster, we obtain a charged-particle multiplicity $\langle n \rangle_{\text{ch}} = 2.7$–$4.0$. Experimentally, $\langle n \rangle_{\text{ch}} \simeq 3.2$.

(C) If we use Eq. (7.7) we can use the bootstrap results of Sec. VI to predict the $K^- p \to \bar{K}^0 X$ inclusive cross section, which is dominated by the Reggeon-Reggeon-Pomeron graph of Fig. 8. This is given by

$$\frac{d\sigma}{dt'dM^2} = \frac{1}{16\pi s^2} \gamma_{KK\alpha}{}^2(t') |X(t')|^2 \times \frac{1}{\sqrt{6}} g_{\alpha\alpha\hat{P}}(t't'0) \gamma_{pp\hat{P}}(0) \times \left(\frac{s}{\bar{M}^2}\right)^{2\alpha(t')} (\bar{M}^2\alpha')^{\alpha_{\hat{P}}(0)}, \tag{7.11}$$

where now $\bar{M}^2 = M^2 - m_p{}^2 - t'$, and $\gamma_{KK\alpha}{}^2 = 2\gamma_{KKf}$ with our normalization. If we again make an end-cluster correction (see Ref. 6 or Appendix C)

$$g_{\alpha\alpha\hat{P}} = \left(\frac{m_N{}^2}{s_a}\right)^{\alpha(0) - \alpha_{\hat{P}}(0)} \frac{\gamma_{\pi\pi\hat{P}}}{\gamma_{\pi\pi f}} g_{\alpha\alpha f}, \tag{7.12}$$

which can be calculated using Eqs. (7.7), (6.3), and (5.7). The remaining parameters can be extracted from two-body processes. Taking $\gamma_{\pi\pi f}\gamma_{ppf} \simeq 20$ (mb-GeV units) and the quark-duality results $\gamma_{ppf} = \frac{3}{2}\gamma_{\pi\pi f} = 3\gamma_{KKf}$, we obtain

$$d\sigma/dt'dM^2 = 0.29 \text{ mb/GeV}^4 \tag{7.13}$$

at $t' = 0$. This should be compared with the experimental value

$$d\sigma/dt'dM^2 = 0.33 \text{ mb/GeV}^4 \tag{7.14}$$

at $t' = -0.1$ GeV^2.

VIII. CONCLUSION

We have considered a dual multiperipheral model and have imposed the Adler PCAC condition

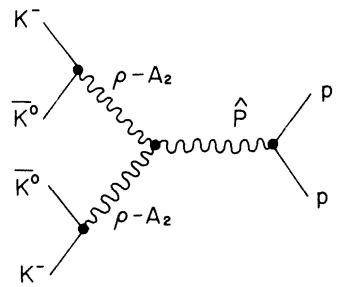

FIG. 8. The dominant graph which contributes to the cross section for $K^- p \to \bar{K}^0 X$ in the triple-Regge region.

and crossing near $s=t=0$. We then obtained the following results:

(i) Our Reggeon intercept is $\alpha(0)\simeq 0.5$.

(ii) The Regge coupling we obtained only has a partial resemblance to the one given by the dual-tree approximation.

(iii) Our Regge couplings and multiplicities are in reasonable accord with experiment.

Further work might involve the following:

(a) Doing a more accurate calculation which does not make the crude approximations used in Sec. V.

(b) Doing a calculation over a wider range of t, positive as well as negative.

(c) Adding in higher clusters,[6,14] including perhaps $\bar{p}$. The latter would also involve baryon exchange.

(d) Imposing alternative or additional crossing conditions.

(e) Imposing crossing directly on the multiperipheral-model absorptive part, using, e.g., Eqs. (3.5) and (3.8).

(f) Applying the Pade approach in an improved way, either by going to higher orders or by summing a different series (see Appendix A).

In the present paper we used a rather simple multiperipheral model with simple resonance clusters. In a more systematic framework,

(A) the multiperipheral cluster-production amplitude could be systematically improved upon, perhaps using Reggeon-calculus techniques,[17]

(B) the clusters could be replaced by entire low-energy (low-J) Regge-Regge "scattering" amplitudes, which would themselves be calculated from multiperipheral ladders plus corrections. Energy thresholds in the Regge exchanges of the multiperipheral chain may have to be put in to avoid double-counting (for low J).

ACKNOWLEDGMENTS

The author would like to thank Professor B. W. Lee and Professor C. Quigg for their hospitality at the Fermi National Accelerator Laboratory, where this work was done. He would also like to thank Dr. G. Thomas and Dr. C. Sorensen for a very helpful discussion.

APPENDIX A: A GENERAL MULTI-REGGE MODEL WITH REGGE-CLUSTER DUALITY

We will give a justification for our use of the [1, 1] Padé approximant (4.7) by considering a general model with Regge-cluster duality. This will also suggest ways of improving our approximation.

We assume that the absorptive part A is given by Fig. 9, where I and II are the initial and final

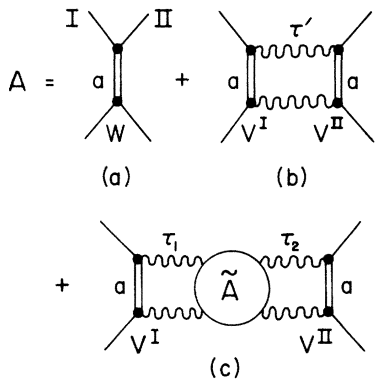

FIG. 9. Absorptive part for a general multi-Regge model.

two-body systems in the t channel. At $t=0$ we then have

$$A_l = W_l + B_l + C_l , \tag{A1}$$

where W, B, and C correspond to Figs. 9(a), 9(b), and 9(c); W is given by Eq. (4.5), whereas

$$B_l = \int \rho d\tau' V_l^{\mathrm{I}}(\tau') k_l(\tau') V_l^{\mathrm{II}}(\tau') \tag{A2}$$

and

$$C_l = \int\int \rho d\tau_1 \rho d\tau_2 V_l^{\mathrm{I}}(\tau_1) k_l(\tau_1) \tilde{A}_l(\tau_1, \tau_2) \times k_l(\tau_2) V_l^{\mathrm{II}}(\tau_2) , \tag{A3}$$

where ρ is a number given by phase space and k_l is a two-Regge propagator. In a simple Chew-Goldberger-Low–type model[18] with thresholds, we would have

$$k_l(\tau) = \frac{\bar{k}(\tau)}{l+1-2\alpha(\tau)} x^{-l-1+2\alpha(\tau)} , \tag{A4}$$

where x is a threshold factor.[7,6]

The "reduced" amplitude $\tilde{A}$ is given by the integral equation of Fig. 10,

$$A_l(\tau_1, \tau_2) = \tilde{V}_l(\tau_1, \tau_2) + \int \rho d\tau' \tilde{V}_l(\tau_1, \tau') k_l(\tau') \tilde{A}_l(\tau', \tau_2) . \tag{A5}$$

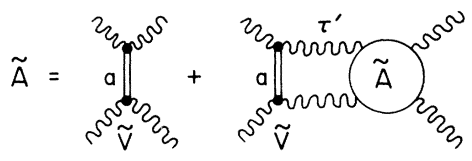

FIG. 10. Integral equation for the absorptive part $\tilde{A}$ for Regge-Regge "scattering."

Our cluster coupling functions are given by Eq. (3.9) and

$$V^i(s,\tau)=\Gamma_i(\tau)\delta(s-s_a),\quad i=\mathrm{I},\mathrm{II} \tag{A6}$$

$$\tilde{V}(s,\tau_1,\tau_2)=\tilde{\Gamma}(\tau_1,\tau_2)\delta(s-s_a), \tag{A7}$$

assuming that all our clusters have the same mass. Cluster-Regge duality, as in Fig. 4 and Eq. (2.4), now gives

$$\Gamma=\gamma_{\mathrm{I}}\gamma_{\mathrm{II}}F_W, \tag{A8}$$

$$\Gamma_i(\tau)=\gamma_i g(\tau)F_V(\tau), \tag{A9}$$

$$\tilde{\Gamma}(\tau_1,\tau_2)=g(\tau_1)g(\tau_2)\tilde{F}_V(\tau_1\tau_2). \tag{A10}$$

Prescription A. If we assume a Regge behavior s^α for $s>N_0$, a simple finite-energy sum rule

$$\int_0^{N_0} ds[A(s,0)-\gamma_{\mathrm{I}}\gamma_{\mathrm{II}}(\alpha' s)^{\bar{\alpha}}]=0, \tag{A11}$$

when combined with Eqs. (3.9) and (3.10), gives

$$\alpha' F_W=(\alpha' N_0)^{\bar{\alpha}+1}/(\bar{\alpha}+1). \tag{A12}$$

Similarly, finite-mass sum rules applied to Regge-particle and Regge-Regge "scattering" give

$$\alpha' F_V(\tau)=(\alpha' s_a)^{2\alpha(\tau)}\frac{(\alpha' N_0)^{\bar{\alpha}+1-2\alpha(\tau)}}{\bar{\alpha}+1-2\alpha(\tau)} \tag{A13}$$

and

$$\tilde{F}_V(\tau_1,\tau_2)=F_V(\tau_2). \tag{A14}$$

Suppose now that we have a factorizable projection formula

$$\tilde{A}_l(\tau_1,\tau_2)=\int ds\,P_l(s,\tau_1)P_l(s,\tau_2)\tilde{A}(s,\tau_1,\tau_2) \tag{A15}$$

and similarly for A. For example, a simple Mellin transform would correspond to

$$P_l(s,\tau_1)P_l(s,\tau_2)=s^{-l-1}. \tag{A16}$$

If we assume that the external particles have negligible mass (as would be the case if they were pions), Eqs. (3.9), (A6)–(A10) would then give

$$W_l=\Gamma P_l^2(s_a,0), \tag{A17}$$

$$V_l^i(\tau)=\Gamma_i(\tau)P_l(s_a,\tau)P_l(s_a,0), \tag{A18}$$

$$\tilde{V}_l(\tau_1,\tau_2)=\tilde{\Gamma}(\tau_1,\tau_2)P_l(s_a,\tau_1)P_l(s_a,\tau_2). \tag{A19}$$

If we assume that $\tilde{F}_V$ factorizes

$$\tilde{F}_V(\tau_1,\tau_2)=f_1(\tau_1)f_2(\tau_2) \tag{A20}$$

as in Eq. (A14) (example A), Eqs. (A10) and (A19) give

$$\tilde{V}_l(\tau_1,\tau_2)=u_l(\tau_1)v_l(\tau_2), \tag{A21}$$

where

$$u_l(\tau)=g(\tau)f_1(\tau)P_l(s_a,\tau), \tag{A22}$$

$$v_l(\tau)=g(\tau)f_2(\tau)P_l(s_a,\tau). \tag{A23}$$

If we iterate Eq. (A5) using Eq. (A21) we obtain

$$\tilde{A}_l(\tau_1,\tau_2)=u_l(\tau_1)v_l(\tau_2)+u_l(\tau_1)K_l v_l(\tau_2)+\cdots, \tag{A24}$$

where

$$K_l=\int \rho d\tau\, v_l(\tau)k_l(\tau)u_l(\tau). \tag{A25}$$

If we sum the series (A24) we obtain

$$\tilde{A}_l(\tau_1,\tau_2)=u_l(\tau_1)v_l(\tau_2)/(1-K_l). \tag{A26}$$

Exactly the same result is obtained if we form the [1, 1] Padé approximant from Eq. (A24).

In practice, it may be more convenient to deal with particle-particle rather than Reggeon-Reggeon scattering. Inserting, therefore, Eq. (A24) into Eq. (A3) we obtain

$$C_l=\gamma_{\mathrm{I}}\gamma_{\mathrm{II}}P_l^2(s_a,0)K_l J_l(1+K_l+K_l^2+\cdots), \tag{A27}$$

where

$$J_l=\int \rho d\tau\, v_l^2(\tau)k_l(\tau). \tag{A28}$$

If we sum Eq. (A27) we obtain

$$C_l=\gamma_{\mathrm{I}}\gamma_{\mathrm{II}}P_l^2(s_a,0)K_l J_l/(1-K_l). \tag{A29}$$

Exactly the same result is obtained if we form the [1, 1] Padé approximant from the series (A27).

One problem with forming Padé approximants for C_l rather than A_l is that it involves the evaluation of diagrams which are of higher order than the box. We can obtain a certain degree of simplification if

$$f_2(\tau)=F_V(\tau), \tag{A30}$$

as would be true, for example, with Eq. (A14) (example A). Then, from Eq. (A2),

$$B_l=\gamma_{\mathrm{I}}\gamma_{\mathrm{II}}P_l^2(s_a,0)J_l. \tag{A31}$$

Combining this with Eq. (A27) we obtain

$$B_l+C_l=B_l(1+K_l+K_l^2+\cdots). \tag{A32}$$

If we sum this series we obtain

$$(B_l+C_l)=B_l/(1-K_l). \tag{A33}$$

Once again, exactly the same result would be obtained if we formed the [1, 1] Padé approximant of the series (A32).

The simpler procedure followed in Sec. IV is somewhat harder to justify. Thus, from Eqs. (A1) and (A33),

$$A_l=\frac{W_l}{1-K_l}\left(1-K_l+\frac{B_l}{W_l}\right). \tag{A34}$$

We see that this agrees with the [1, 1] approximant of Eqs. (4.7) and (4.8) only if

$$K_l \simeq B_l/W_l . \tag{A35}$$

To see whether this may be satisfied, we note from Eqs. (A31), (A17), (A8), and (A25) that we can write

$$B_l/W_l = F_W^{-1} \int \rho d\tau\, v_l^2(\tau) k_l(\tau) \tag{A36}$$

and

$$K_l = F_W^{-1} \int \rho d\tau\, v_l^2(\tau) k_l(\tau) R(\tau) , \tag{A37}$$

where

$$R(\tau) = F_W \tilde{F}_V(\tau, \tau)/F_V^2(\tau) . \tag{A38}$$

We then have two options:

(i) We could first write down an expression for B_l/W_l. By comparing Eqs. (A36) and (A37) we then see that we can obtain an expression for K_l simply by inserting the factor $R(\tau)$ into the integral. We can then calculate A_l from Eq. (A34). It is straightforward to generalize this prescription to $t \neq 0$.

(ii) We could actually check whether $R(\tau) \approx 1$, since this leads immediately to Eq. (A35).

Prescription B. Instead of prescription A, we will assume the Regge behavior $\nu^{\bar{\alpha}}$ (for $s > N_0$) which is normally used in finite-energy sum rules; ν is the same sort of crossing-symmetric variable which we encountered in Sec. III. We then have

$$\alpha' F_W = (\alpha' N_0)^{\bar{\alpha}+1}/(\bar{\alpha}+1) , \tag{A39}$$

$$F_V(\tau) \simeq \alpha'^{\bar{\alpha}} (s_a - \tau)^{2\alpha(\tau)} \frac{(N_0 - \tau)^{\bar{\alpha}+1-2\alpha(\tau)}}{\bar{\alpha}+1-2\alpha(\tau)} , \tag{A40}$$

$$\tilde{F}_V(\tau_1, \tau_2) = \alpha'^{\bar{\alpha}} (s_a - \tau_1 - \tau_2)^{2\alpha(\tau_2)} \times \frac{(N_0 - \tau_1 - \tau_2)^{\bar{\alpha}+1-2\alpha(\tau_2)}}{\bar{\alpha}+1-2\alpha(\tau_2)} . \tag{A41}$$

The last expression is not exactly factorizable. For small τ_1 and τ_2, however, we can write

$$\tilde{F}_V(\tau_1, \tau_2) \simeq f_1(\tau_1) F_V(\tau_2) , \tag{A42}$$

where

$$f_1(\tau_1) \simeq 1 - \tau_1 \left[\frac{\bar{\alpha}+1-2\alpha(0)}{N_0} + \frac{2\alpha(0)}{s_a} \right] + \cdots . \tag{A43}$$

Since this is the dominant region within our integrals the above formalism continues to apply.

In Secs. II and III we argued that a formula such as Eq. (3.15) is more appropriate than Eq. (A39) for relating Γ to $\gamma_I \gamma_{II}$. If we therefore make the substitution

$$F_W \to F \tag{A44}$$

in Eq. (A39) and plot $R(\tau)$ with $\bar{\alpha} = \alpha(0) = 0.5$ and $N_0 = 1$, we do in fact find that $R(\tau) \simeq 1$ (see Fig. 11). From Eqs. (A36) and (A37), this in turn means that Eq. (A35) is satisfied and that the [1, 1] approximant of Eqs. (4.7) and (4.8) is a good approximation.

APPENDIX B: EXPLICIT PION-EXCHANGE MODEL

All of the formulas listed in Appendix A are valid in the case of the Amati-Bertocchi-Fubini-Stanghellini-Tonin model.[19] In particular we obtain Eq. (A5) with

$$\rho = \tfrac{1}{16}\pi^3 , \tag{B1}$$

$$k_l^{-1}(\tau) = (m_\pi^2 - \tau)^2 (l+1) , \tag{B2}$$

provided we make an $O(1, 3)$ partial-wave projection of the off-shell absorption part[20]

$$\tilde{A}_l(\tau_1, \tau_2) = \int ds\, e^{-(l+1)\theta(s,\tau_1,\tau_2)} \tilde{A}(s, \tau_1, \tau_2) , \tag{B3}$$

where

$$e^{-\theta(s,\tau_1,\tau_2)} = 2(\tau_1\tau_2)^{1/2} \{ (s - \tau_1 - \tau_2) + [(s - \tau_1 - \tau_2)^2 - 4\tau_1\tau_2]^{1/2} \}^{-1} . \tag{B4}$$

In this model, of course,

$$A_l = \tilde{A}_l(m_\pi^2, m_\pi^2) . \tag{B5}$$

The projection (B3) does not have the factorizable form of (A15). It is a good approximation, however, to replace Eq. (B4) by

$$e^{-\theta(s,\tau_1,\tau_2)} \simeq s(\tau_1\tau_2)^{1/2} (s - \tau_1)^{-1} (s - \tau_2)^{-1} . \tag{B6}$$

Equation (B3) then has the form of (A15) with

$$P_l(s, \tau) = [(-s\tau)^{1/2}/(s - \tau)]^{l+1} . \tag{B7}$$

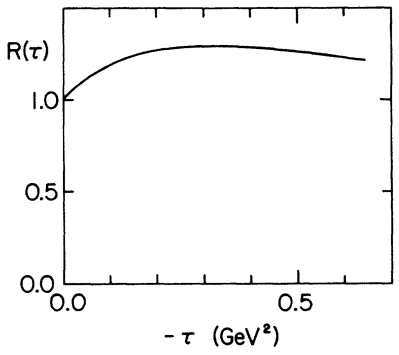

FIG. 11. Plot of the factor $R(\tau)$ given by Eqs. (A38) and (A44).

Explicit calculations have shown that the resulting solution of Eq. (A5) is accurate to within about 10% for physically relevant values of the input parameters.[21]

As in Appendix A, the [1,1] Padé approximant is valid provided Eqs. (A20) and (A30) apply and $R \simeq 1$. We will consider two separate cases:

(i) If we make the traditional assumption of scalar clusters we do not have duality in the usual sense. Formally we can still write down Eqs. (A8)–(A10) with

$$F_W = F_V(\tau) = \tilde{F}_V(\tau_1, \tau_2) = \text{constant}, \tag{B8}$$

even though the γ_i and g do not have their usual meaning; we have $g(\tau) = \text{constant}$. From Eq. (B8), we find that Eqs. (A20) and (A30) apply and that $R = 1$, so that the [1,1] approximant is justified.

(ii) If we assume cluster-Regge duality we again have Eqs. (A39)–(A43) but this time with

$$\bar{\alpha} = 0.5, \quad \alpha(\tau) = 0, \text{ all } \tau, \tag{B9}$$

since we are dealing with an elementary pion. We again find that Eqs. (A20) and (A30) apply, and that $R \simeq 1$, so that the [1,1] approximant is again justified.

APPENDIX C: END-CLUSTER EFFECTS IN A SIMPLE MODEL

Suppose the end clusters in Figs. 9(b) and 9(c) are different from cluster a. Equation (A7) is then the same, but we must replace Eq. (A6) by

$$V^i(s,\tau) = \Gamma_i(\tau)\delta(s - s_i), \quad i = \text{I, II} \tag{C1}$$

with $s_i \neq s_a$. We will, however, assume that the τ dependences of the Γ_i are the same as in $\pi\pi$ scattering, where $s_i = s_a$. The expressions for $\tilde{A}_l$ are then the same as before, but now

$$C_l = \frac{\Gamma_{\rm I}(0)\Gamma_{\rm II}(0)}{\Gamma_{\rm I}^{\pi\pi}(0)\Gamma_{\rm II}^{\pi\pi}(0)} \left(\frac{s_{\rm I}s_{\rm II}}{s_a^{\,2}}\right)^{-l-1} C_l^{\pi\pi} \tag{C2}$$

if we use the Mellin-transform projection (A16) and (A15). If we now calculate the residue of the pole in C_l at $l = \alpha$ coming from the vanishing of the universal denominator $(1 - K_l)$, we obtain

$$b = \frac{\Gamma_{\rm I}(0)\Gamma_{\rm II}(0)}{\Gamma_{\rm I}^{\pi\pi}(0)\Gamma_{\rm II}^{\pi\pi}(0)} \left(\frac{s_{\rm I}s_{\rm II}}{s_a^{\,2}}\right)^{-\alpha-1} b^{\pi\pi}, \tag{C3}$$

a result which applies to both f and $\hat{P}$. It we take the ratio of the two, we obtain a modified version of f/P universality

$$\frac{b_{\hat{P}}}{b_f} = \left(\frac{s_{\rm I}s_{\rm II}}{s_a^{\,2}}\right)^{\alpha_f - \alpha_{\hat{P}}} \frac{b_{\hat{P}}^{\pi\pi}}{b_f^{\pi\pi}}. \tag{C4}$$

This result is also valid for $t \neq 0$.[6]

It is straightforward to derive an expression for the average multiplicity in this model. Now for large s

$$\sigma_{\rm tot} = \sum_n \sigma_n \phi^n \simeq b s^{\alpha - 1}, \tag{C5}$$

where $\sigma_n \phi^n$ is the partial cross section for the production of n clusters, and ϕ is the same parameter as in Sec. IV. Then

$$\langle n \rangle_{\rm cluster} = \sigma_{\rm tot}^{-1} \sum_n n \sigma_n \phi^n \tag{C6}$$

$$= \sigma_{\rm tot}^{-1}\, \phi \frac{\partial}{\partial \phi} \sigma_{\rm tot} \tag{C7}$$

$$= \sigma \left(\frac{1}{b} \frac{\partial b}{\partial \phi} + \frac{\partial \alpha}{\partial \phi} \ln s \right). \tag{C8}$$

If the dominant exchange is the $\hat{P}$ we have Eq. (7.9). If we use Eq. (C3) we obtain

$$\langle n \rangle_{\rm cluster} = \phi \left(\frac{1}{b_{\hat{P}}^{\pi\pi}} \frac{\partial b_{\hat{P}}^{\pi\pi}}{\partial \phi} + \frac{\partial \alpha_{\hat{P}}}{\partial \phi} \ln \frac{s s_a^{\,2}}{s_{\rm I} s_{\rm II}} \right). \tag{C9}$$

APPENDIX D: DIRECT IMPOSITION OF ADLER ZERO

We will now give a simple example of how the Adler-zero condition (3.5) could be directly imposed on a multiperipheral amplitude. A broad class of multiperipheral models gives the form

$$A_l(t) = n_l(t)/[1 - K_l(t)], \tag{D1}$$

where n_l is nonsingular in l and

$$K_l \propto \ln[l - \alpha_c(t)] \tag{D2}$$

for l in the neighborhood of $\alpha_c(t) = 2\alpha(\frac{1}{4}t) - 1$. Thus, when $l \to \alpha_c$, $K_l \to \infty$ and so $A_l \to 0$. If we identify this zero with that of Eq. (3.5) we see that we must have $\alpha_c(0) = 2\alpha(0) - 1 = 0$, so that $\alpha(0) = 0.5$.

The above argument cannot, of course, be applied to a realistic planar amplitude, for which n_l must also have a branch point at $l = \alpha_c$. Indeed it has been argued[4] that this cut must be such as to cancel the cut in K_l. However, suppose we add a cylinder correction. With the usual factorization assumptions (see, e.g., Ref. 5), we then have

$$A_l = A_l^{\rm Pl} + A_l^{\rm Pl} K_l^X A_l^{\rm Pl} + \cdots = A_l^{\rm Pl}/(1 - K_l^X A_l^{\rm Pl}), \tag{D3}$$

where $A_l^{\rm Pl}$ is the planar amplitude and K_l^X is the cylinder "propagator," which can be expected to have a singularity similar to (D2). If $A_l^{\rm Pl}$ is nonsingular at $l = \alpha_c$, Eq. (D3) then has the same sort of structure as (D1), and so we again conclude that $\alpha(0) = 0.5$.

*Work supported in part by ERDA.
†Operated by Universities Research Association Inc. under contract with the Energy Research and Development Administration.

[1]G. Veneziano, Nucl. Phys. B74, 365 (1974); Phys. Lett. 52B, 220 (1974).
[2]Chan Hong-Mo, J. E. Paton, and Tsou Sheung-Tsun, Nucl. Phys. B86, 479 (1975); Chan Hong-Mo, J. E. Paton, Tsou Sheung-Tsun, and Ng Sing Wai, *ibid.* B92, 13 (1975).
[3]C. Rosenzweig and G. Veneziano, Phys. Lett. 52B, 335 (1974); M. M. Schaap and G. Veneziano, Lett. Nuovo Cimento 12, 204 (1975); J. Kwiecinski and N. Sakai, Nucl. Phys. B106, 44 (1976); Ken-ichi Konishi, Nucl. Phys. B116, 356 (1976).
[4]M. Bishari and G. Veneziano, Phys. Lett. 58B, 445 (1975).
[5]Huan Lee, Phys. Rev. Lett. 30, 719 (1973); G. Veneziano, Phys. Lett. 43B, 413 (1973); Chan Hong-Mo, and J. E. Paton, *ibid.* 46B, 228 (1973); C. Rosenzweig and G. F. Chew, *ibid.* 58B, 93 (1975); Nucl. Phys. B104, 290 (1976); C. Schmid and C. Sorensen, *ibid.* B96, 209 (1975); N. Papadopoulos, C. Schmid, C. Sorensen, and D. M. Webber, *ibid.* B101, 189 (1975).
[6]L. A. P. Balázs, Phys. Rev. D 15, 309 (1977); Phys. Lett. 61B, 187 (1976).
[7]G. F. Chew and D. Snider, Phys. Lett. 31B, 75 (1970); G. F. Chew and J. Koplik, *ibid.* 48B, 221 (1974).
[8]L. A. P. Balázs, Phys. Rev. D 2, 999 (1970); Phys. Lett. 29B, 228 (1969).
[9]L. A. P. Balázs, Phys. Rev. D 15, 319 (1977).
[10]S. Adler, Phys. Rev. 137, B1022 (1965).
[11]C. Lovelace, Phys. Lett. 28B, 264 (1968).
[12]G. A. Baker, Jr., *Essentials of Pade Approximants* (Academic, New York, 1975).
[13]J. Zinn-Justin, Phys. Rep. 1C, 55 (1971).
[14]J. Dash, Phys. Lett. 61B, 199 (1976); J. Dash and S. T. Jones, Nucl. Phys. B120, 345 (1977).
[15]J. Dash, Phys. Rev. D 9, 200 (1974); N. Bali and J. Dash, *ibid.* 10, 2102 (1974); C. Quigg and E. Rabinovici, *ibid.* 13, 2525 (1976); P. R. Stevens, G. F. Chew, and C. Rosenzweig, Nucl. Phys. B110, 355 (1976).
[16]P. D. B. Collins and F. D. Gault, Nucl. Phys. B113, 34 (1976).
[17]H. D. I. Abarbanel, J. D. Bronzan, R. L. Sugar, and A. R. White, Phys. Rep. 21C, 119 (1975).
[18]G. F. Chew, M. L. Goldberger, and F. E. Low, Phys. Rev. Lett. 22, 208 (1969).
[19]D. Amati, A. Stanghellini, and S. Fubini, Nuovo Cimento 26, 896 (1962); L. Bertocchi, S. Fubini, and M. Tonin, *ibid.* 25, 626 (1962).
[20]S. Nussinov and J. Rosner, J. Math. Phys. 7, 1670 (1966).
[21]Chun-Fai Chan and B. R. Webber, Phys. Rev. D 5, 933 (1972).